RSC Advances

ROYAL SOCIETY OF CHEMISTRY

www.rsc.org/advances

Journal Name

ARTICLE

Self-assembly, Photoresponsive Behavior and Transport Potential of Azobenzene Grafted Dendronized Polymeric Amphiphiles

Meena Kumari,[a] Muriel Billamboz,[b] Estelle Leonard,[b] Christophe Len,[b,c*] Christoph Böttcher,[e] Ashok K. Prasad,[a] Rainer Haag[d] and Sunil K. Sharma[a,*]

Photoresponsive polymeric amphiphiles were developed by first synthesizing the polyester chain *via* Novozym 435 catalyzed step growth, condensation polymerization of poly[ethylene glycol bis(carboxymethyl) ether]diethylester and 2-azidopropan-1,3-diol followed by its grafting with 4'-butyl-4-propargyloxy(azobenzene) and [G2.0] polyglycerol dendron by using 'Click chemistry' approach. The resulting polymers were observed to form supramolecular micellar aggregates in the aqueous solution. The critical aggregation concentration (CAC) was determined *via* fluorescence measurements and using 'Nile red' as a probe. The nano-structures formed in the aqueous solution were characterized by dynamic light scattering (DLS) and cryo-TEM measurements. The encapsulation potential of polymeric amphipihiles for Nile red and curcumin as well as their release via *trans-cis* photoisomerization of the embedded azobenzene moiety was studied, by absorbance and fluorescence spectroscopy techniques. The developed polymeric micellar systems behave as efficient photoresponsive smart nanocarriers.

Received 00th January 20xx,
Accepted 00th January 20xx

DOI: 10.1039/x0xx00000x

www.rsc.org/

Introduction

In recent years, stimuli responsive polymeric materials have attracted significant attention due to their potential applications in the field of optical devices like liquid-crystal displays, molecular switches, nano- sensors, drug delivery and gene transport systems.[1] The stimuli responsive behavior of polymeric nano-structures depends on a number of stimuli which include light, pH, temperature, ionic strength, various chemicals, electric and magnetic fields.[2] The development of photoresponsive smart materials whose properties can be reversibly modulated by light have also gained immense attention.[3] Light has been most commonly used stimuli for controlling the release of entrapped materials from nano assemblies because of its precise control over structural change.[4] Using light as stimuli, various strategies have been applied for controlling the release from nanovectors.[5] In that case, the isomerization of photo sensitive groups specially azobenzene constitute an interesting approach.[6-8] Out of various photochromic systems available, azobenzene is the most frequently used chromophore because of its convenient synthesis, ability to induce the pre-association of surfactant monomers even below the CMC,[9] and potential to undergo rapid, reversible and very efficient *trans-cis* photoisomerization.[10] The azobenzene isomerization is accompanied by significant changes in the absorption spectrum, dipole moment, refractive index, dielectric constant and other optical, geometrical, mechanical and chemical properties which are then transferred to the large host systems having them.[11,12] The photo induced geometrical isomerization of azobenzene has also proved to be very effective even in strong constraints,[13] when it is embedded in supramolecular structures like films,[14] vesicles[15]

[a] Department of Chemistry, University of Delhi, Delhi-110007, India
Fax: +91-11-27666950; Email: sksharma@chemistry.du.ac.in

[b] Sorbonne Universités, Université de Technologie de Compiègne, Ecole Supérieure de Chimie Organique et Minérale, Centre de Recherche Royallieu, CS 60319, F-60203 Compiègne, France; Email: christophe.len@utc.fr

[c] Department of Chemistry, University of Hull, Hull, HU6 7RX, England

[d] Institut für Chemie und Biochemie, Freie Universität Berlin, Takustrasse 3, 14195 Berlin, Germany

[e] Forschungszentrum für Elektronenmikroskopie, Institut für Chemie und Biochemie, Freie Universität Berlin, Fabeckstraße 36a, 14195 Berlin, Germany

Electronic Supplementary Information (ESI) available. See DOI: 10.1039/x0xx00000x

rods,[15] micelles,[16] of polymeric scaffolds. These supramolecular structures are derived by non-covalent interactions, thus avoid complicated synthetic procedures.[4] The photoresponsive azobenzene moiety plays a key role in the formation and disorganization of supramolecular architectures. The wavelength affecting this geometrical transformation can also be tuned by varying the substituents and other auxochromes to the main chromophore.[10] A large number of polymeric scaffolds have been synthesized with an azobenzene moiety either in the main chain[17,18] or in the side chain.[19,20] However, the polymers having azobenzene moieties in the side chain have attracted much attention because of their unique properties.[20] Such polymers bear an additional advantage of exhibiting the photoresponsive behavior even at lower content of azobenzene as compared to their azo analogs having azobenzene units in the main chain. This has been explained by the enhanced segregation ability of block co-polymers due to azobenzene-azobenzene interactions at the nanoscale level, resulting in the well defined structures.[14,21] Herein, we have synthesized PEG and azido glycerol based dendronized and non-dendronized polymeric systems having azobenzene moiety and [G2.0] polyglycerol (PG) dendron grafted on copolymer chain. The immobilized *Candida antarctica* lipase (Novozym 435) was used for synthesizing the base co-polymer from poly[ethylene glycol bis(carboxymethyl) ether]diethylester ($\overline{M}_n$: 1000 g/mol) and azido glycerol via transesterification reaction under solventless conditions, developed by our group.[22-27] The azido group of the base co-polymer was used for further functionalization using 'grafting to' approach via copper (I) catalyzed Huisgen-1,3-dipolar cycloaddition reaction,[28] with 4'-butyl-4-propargyloxy(azobenzene) (**2**) and propargylated [G2.0] polyglycerol dendron (**3**), synthesized separately. The resulting polymeric systems were fully characterized and observed to self-assemble in the aqueous medium above the critical aggregation concentration (CAC), forming supramolecular architectures that closely resemble the micelles/micellar aggregates. The particle size and the CAC in the aqueous solution were determined by using the dynamic light scattering (DLS) supplemented by cryo-TEM and fluorescence measurements using 'Nile red' as a probe, respectively. The *trans-cis* photoisomerization of azo group in both the polymers was studied through absorbance spectroscopy in the aqueous solution, above the CAC values by irradiating at 365 nm. The kinetics of isomerization was compared by calculating their rate constants. The encapsulation potential of these polymers was evaluated for Nile red and curcumin but quantified for former only. The effect of *trans-cis* geometrical isomerization of azobenzene moiety was also evaluated on the release behavior of encapsulated guest. Nile red being a solvatochromic dye,[29,30] is a most frequently used probe for studying the photo-controlled release using fluorescence spectroscopy. *Trans-cis* isomerization is mainly caused by the irradiation with UV light (approx. 350-400 nm)[5,31-38] while *cis-trans* isomerization could occur either thermally by keeping the samples in dark[31,33,34] or by irradiating them using visible light[32,36-38] or with UV light (approx. 250-300 nm).[9,39] The *trans-cis* isomerization mainly leads to an increase in dipole moment with the subsequent reduction in fluorescence intensity of Nile red, while the reverse occurs for the *cis-trans* isomerization. This is the most commonly used strategy for azopolymeric systems to study their release potential. The majority of the systems has reported the decrease in the fluorescence intensity of Nile red on *trans* to *cis* isomerization, however the literature suggests a lot of variation in the regain of fluorescence intensity due to re-encapsulation of the dye on subjecting the system to *cis-trans* isomerization either thermally or photochemically. Yu's group has synthesized azobenzene functionalized block co-polymers, responsive to both temperature and light which showed a complete regain of fluorescence intensity of Nile red in 20 s up to 9 cycles of *trans-cis-trans* reverse isomerization.[36] Oriol *et al.* have synthesized amphiphilic linear-dendritic block copolymers (LSBCs) by linking poly(ethylene glycol) on one end and 4-isobutyloxyazobenzene (AZO)/ hydrophobic chain (C_{18}) on the other end of fourth generation, 2,2-di(hydroxymethyl)propionic acid (bis-MPA) based dendron, with varying composition of hydrophobic content i.e., PEG-*b*-d(isoAzo/C18) - 25/75, 75/25 and 50/50.[33] They have reported that low content of azo moiety accelerates the rate of geometrical isomerization without any release of encapsulated Nile red while the release was triggered by increasing the azo content. A complete regain in the fluorescence intensity of Nile red on *cis-trans* isomerization keeping the UV irradiated solutions in dark for 24 h was observed for PEG-*b*-d(isoAzo/C18) - 25/75 while a partial regaining in fluorescence intensity leading to net release of encapsulated material was reported for PEG-*b*-d(isoAzo/C18) - 75/25 and 50/50 systems.[33] Also, they have reported an another miktoarm copolymeric system having azobenzene moiety that

showed complete regain in the fluorescence intensity of Nile red.[34] However few other groups have emphasized the stirring effect along with the conditions required for *cis-trans* isomerization (photochemical or thermal restoration in dark) for regaining the fluorescence intensity of Nile red e. g. Das *et al.* have developed azobenzene based co-polymers forming spherical aggregates which showed only 50 % regain in the fluorescence intensity of Nile red on photochemical *cis-trans* isomerization while it was completely restored by keeping the UV-irradiated solution in dark for 3 days with constant stirring.[37] Xu's group has explained the partial regain in fluorescence intensity of Nile red for azobenzene functionalized polymeric systems, on *trans-cis-trans* reverse isomerization, on the basis of higher rate of micelle formation compared to drug loading.[38] Lafleur's *et al.* has created non-phospholipid photosensitive liposomes which showed switchable photo-controlled release of Sulforhodamine B (SRB), on applying photo-cycles of alternate UV (350 nm) and visible light (450 nm).[5] They have shown that release from SRB encapsulated liposomes could be initiated on irradiating with 350 nm light for 120 or 150 s and continues further without prolonged irradiation and could be stopped when desired by irradiating at 450 nm for 180 s thereby achieving the precisely controlled release.[5] The systems which regain the fluorescence intensity of encapsulated dye on *trans-cis-trans* isomerization are reported to find applications in sensor technologies and catalytic systems,[36] while the systems having partial regain indicate photoresponsive release and could find potential applications as carriers for drug delivery.[5,33,34,35,38] Herein, we have studied the release profile of Nile red on *trans-cis-trans* photoisomerization as a function of photo-cycles using fluorescence spectroscopy for our recently developed azobenzene functionalized polymeric systems.

Experimental section

Materials

All the chemicals and solvents used were purchased from Spectrochem Pvt. Ltd., India and Sigma Aldrich Chemicals Pvt. Ltd., USA. Immobilized *Candida antartica* lipase (Novozym 435) was obtained from Julich Chiral Solutions GmbH (Jülich, Germany). Nile red with purity higher than 98% was purchased from Fluka Chemie GmbH, (Buchs, Switzerland). The solvents were distilled prior to use. The progress of the reactions was monitored by using precoated TLC plates (Merck silica gel 60 F_{254}) and silica gel (100-200) mesh size was used for column chromatography. The spots on the TLC were visualized by using Cerric solution. The dialysis for purification of polymers was performed by using benzoylated dialysis tubing (MW cut off 2,000 Da), purchased from Sigma-Aldrich. Milli-Q water was used for preparing samples for physico-chemical characterization and transport analysis.

Instrumentation

Infrared spectra (IR) of neat samples were recorded using a Perkin-Elmer FT-IR model 9 spectrometer. The ^{1}H, ^{13}C, and ^{2}D HETCOR NMR spectra were recorded on JEOL 400 MHz spectrometer and calibrated using the residual solvent peaks. The chemical shift values are on δ scale. The molecular weights $\overline{M}_w$, $\overline{M}_n$, $\overline{M}_z$ and PDI (polydispersity index) of polymers were determined using an Agilent GPC system equipped with Agilent 1100 pump, refracti index detector, and PLgel columns. THF was used as an eluent at a flow rate of 1.0 mL/min and molecular weights were calibrated using polystyrene standards. CAC of the polymers was determined by fluorescence method using 'Nile red' as a model dye.[40] A stock solution of Nile red was made by dissolving 0.3 mg of Nile red in 1mL of ethanol to form 9.4 x 10^{-4} M solution. The Nile red solution (10 µL) was taken into empty vials and the ethanol was evaporated completely. The polymer solutions of different concentrations (0.25 mM to 0.12 mM) were also prepared up to 2 mL using 1X PBS buffer. These polymer solutions were allowed to stir for 1 h and then transferred to the vials having Nile red in the same sequence and allowed to stir overnight. The final concentration of Nile red was kept at 4.7 x 10^{-6} M. All the solutions were filtered using 0.45 µm polytetrafluoroethylene (PTFE) filter to remove non-encapsulated dye. The fluorescence spectra was recorded for the filtered clear solutions and the fluorescence data (ʎ: 636 nm) obtained was plotted with the log [polymer concentration] for different samples to obtain the CAC values. Malvern Zetasizer Nano ZS analyzer integrated with 4 mW He–Ne laser, λ: 633 nm based on back scattering detection (scattering angle θ = 173°) using an avalanche photodiode detector was used for characterizing the nanostructures (micelles/micellar aggregates) formed in the aqueous solution. The Zetasizer is equipped with a thermostated sample chamber. The samples were prepared in Milli-Q water at a concentration of 10 mg/mL, well above their CACs, by vigorous stirring for 20 h. The samples were filtered using 0.45 µm PTFE filter and equilibrated for 1 h at room temperature before the

measurements. The size of the nano-particles formed from polymer **4a** in the aqueous solution was also evaluated by Cryo-TEM image using a Tecnai F20 transmission electron microscope (FEI company, Oregon, USA) operated at 160 kV accelerating voltage. For cryo preparation, droplets of the sample solution were applied to 1-µm hole diameter perforated carbon film, covered with 200 mesh grids (R1/4 batch of the Quantifoil Micro Tools GmbH, Jena, Germany), which had been hydrophilized before use. The supernatant fluid was removed with a filter paper until an ultra thin layer of the sample solution spanned the holes of the carbon film. The samples were immediately vitrified by propelling the grids into liquid ethane at its freezing point (90 K) with a guillotine-like plunging device. The vitrified samples were then transferred to the microscope using a Gatan (Gatan, Inc., California) cryoholder and stage (model 626). The samples were kept at a temperature of 94 K. Imaging was performed using the low-dose protocol of the microscope at a calibrated primary magnification of 62,000x with the defocus set to 1.8 µm. Data were recorded by an Eagle 4k CCD-camera set to binning factor 2. The Nile red and curcumin encapsulation was studied by using UV and fluorescence spectra measurements. The curcumin was used in excess for encapsulation but quantification could not be done because of overlap of its absorbance spectra with that of polymers. The encapsulation of curcumin was done by following the solid dispersion method.[41] The Nile red encapsulation was studied quantitatively along with its release triggered by photo irradiation with the help of UV and fluorescence spectroscopy. The Nile red encapsulation was done by following the film method.[42] For that, 0.12 mg of Nile red was dissolved in a minimum amount of anhydrous THF and the solvent was allowed to evaporate so that a uniform layer of Nile red was obtained at the bottom of the vial. Then, 1 ml of aqueous polymer solution in 1X PBS buffer (having a concentration of 1 mg/ml) was added to the vial having the thin film of Nile red. The final concentration of dye in the sample for encapsulation becomes 0.4 mM which is then stirred for 20 h. The non-encapsulated fraction of Nile red was removed by filtering it (twice), slowly through 0.45 µm pore size PTFE filter. The Nile red encapsulated samples were lyophilized and re-dissolved in anhydrous methanol for quantification. The absorbance (200-800 nm) spectra were recorded using Cary-300 series UV-vis spectrophotometer from Agilent Technologies in a thermostated UV cell (1 cm). Fluorescence emission spectra (450-800 nm) were recorded from Cary Eclipse fluorescence spectrophotometer using a variable slit system from 575-800 nm for Nile red, and 450 to 700 nm for curcumin. For recording fluorescence emission spectra, the excitation was done at 550 nm for Nile red, and at 420 nm for curcumin with excitation and emission slit set at 5 nm. Microsoft Excel® and Origin 6 softwares were used for data analysis.

Synthetic Procedures

The ester and triazole based polymeric amphiphiles (**4a** and **4b**) were synthesized by following the 'Grafting-to' approach (**Scheme 1**).

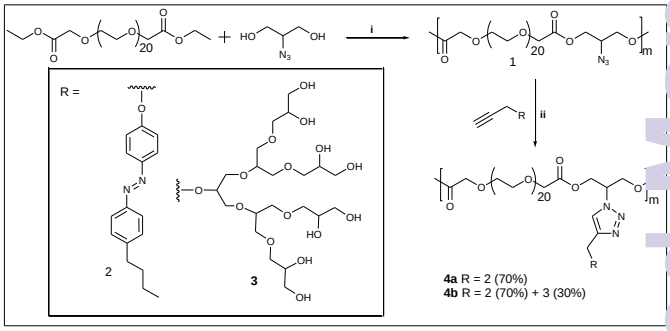

Scheme 1. Synthesis of azobenzene functionalized polymer and its dendronized analog: (i) Novozym 435, 80 °C, vacuum, 60 h; (ii) $[Cu(PPh_3)_3]Br$, DIPEA, DCM/DMF.

Synthesis of 4'-Butyl-4-propargyloxy(azobenzene), 2. 4'-Butyl-4-azophenol was prepared by following the literature procedure.[43] ^1H NMR (400 MHz, $CDCl_3$, δ): 7.86 (d, *J* = 9.26 Hz, 2H, H-2' & H-6'), 7.80 (d, *J* = 8.55 Hz, 2H, H-2 & H-6), 7.30 (d, *J* = 8.56 Hz, 2H, H-3' & H-5'), 6.93 (d, *J* = 9.16 Hz, 2H, H-3 & H-5), 2.69 (t, *J* = 7.99 Hz, 2H), 1.63 (q, *J* = 7.96 Hz, 2H), 1.38 (s, *J* = 7.32 Hz, 2H), 0.93 (t, *J* = 7.32 Hz, 3H); ^{13}C NMR (100.5 MHz, $CDCl_3$, δ): 158.1, 150.9, 147.1, 145.9, 129.0, 124.8, 122.5, 115.7, 35.5, 33.4, 22.3, 13.9.

In a microwave vial were introduced 4'-butyl-4-azophenol (1.016 g, 4 mmol), KOH (448 mg, 8 mmol), water (10 mL) and propargyl bromide (0.90 mL, 8 mmol). The vial was cap-sealed and the mixture was heated at 70°C for 15 min under the microwave. Then, after the extraction with ethyl acetate (3 x 20 mL) and evaporation of the solvent, the crude mixture was purified on flash chromatography on silica gel cartridge (40 g) with cyclohexane/ethyl acetate (100/0 to 70/30) to afford pure 4'-butyl-4-propargyloxy(azobenzene) (768 mg) in 66% yield. IR (Neat): 3447.84, 3274.80, 2928.14, 2857.83, 2129.53, 1599.82, 1585.4, 1497.76, 1458.05, 1376.34, 1297.81, 1233.05, 1144.96, 1107.03, 1017.14, 840.78, 707.12, 677.65, 530.26 cm^{-1}; ^1H NMR (400 MHz, $CDCl_3$, δ): 7.92 (d, *J* = 9.16 Hz, 2H, H-2' & H-6'), 7.82 (d, *J* = 8.52 Hz

2H, H-2 & H-6), 7.32 (d, *J* = 8.56 Hz, 2H, H-3' & H-5'), 7.10 (d, *J* = 9.16 Hz, 2H, H-3 & H-5), 4.78 (d, *J* = 2.44 Hz, 2H, H-1''), 2.70 (t, *J* = 7.96 Hz, 2H, H-1'''), 2.57 (t, *J* = 2.44 Hz, 1H, H-3''), 1.68 (q, *J* = 7.96 Hz, 2H, H-2'''), 1.43 (s, *J* = 7.32 Hz, 2H, H-3'''), 0.91 (t, *J* = 7.32 Hz, 3H, H-4'''); ^{13}C NMR (100.5 MHz, $CDCl_3$, δ): 159.5, 150.9, 147.6, 145.9, 129.0, 124.4, 122.5, 115.1, 78.0, 75.9, 55.9, 35.5, 33.4, 22.3, 13.9; HRMS $[M+H]^+$: calculated 293.1654, found 293.1653.

Synthesis of Propargylated [G2.0] PG Dendron, 3. Propargylated [G2.0] (**3**) polyglycerol dendron was synthesized according to the published procedure.[25,44]

Synthesis of Ester Based Block Co-polymer, 1. The block co-polymer **1** was synthesized from 'bio-catalytic' polymerization of poly[ethylene glycol bis(carboxymethyl) ether]diethylester (M_n: 1000 g/mol) and 2-azidopropane-1,3-diol using Novozym 435 under solventless conditions by following the reported procedure[26,27] and characterized by comparing with the literature data.

Synthesis of Polymeric Amphiphiles, 4a and 4b. The base polymer **1** was functionalized with 4'-butyl-4-propargyloxy(azobenzene) (**2**) (70 %) using 'Click approach' to result in polymer **4a**. While the dendronized analog, **4b** was synthesized by functionalizing with 30 % propargylated [G2.0] PG dendron (**3**) and 70 % 4'-butyl-4-propargyloxy(azobenzene) (**2**) following the 'Click approach' (**Scheme 1**).

General Procedure. Polymer **1** (0.44 mmol) and 4'-butyl-4-propargyloxy(azobenzene) (**2**)/ propargylated [G2.0] polyglycerol dendron (**3**) were taken in a 100 mL flask and dissolved in anhydrous dichloromethane/dimethylformamide (60 mL) under a nitrogen atmosphere. Then tris(triphenylphosphine)copper (I) bromide (0.011 mmol) (0.025 eq.) and DIPEA (2.74 mmol) (6.24 eq.) were added and the reaction mixture was stirred for 48 h at room temperature. IR was used for monitoring the progress of the reaction. The solvents were removed and the product was washed with hexane (by sonication) to remove non-polar reactants and residual copper catalyst, tris(triphenylphosphine)copper (I) bromide. The residual reactants and traces of copper catalyst were removed by dialysis using 2,000 MWCO dialysis tubing, against chloroform for 48 h. The solvent was changed at intervals of 8 h to yield the purified final functionalized polymers, **4a** and **4b**.

Non-dendronized Polymer 4a (70 % Azobenzene Functionalized). Compound **2 (**0.31 mmol) (0.7 eq.) was used in dicholomethane to synthesize polymer **4a** as a viscous oil in 87% yield. IR (Neat): 3431.16, 2919.94, 2871.83, 2125.67, 1751.69, 1641.27, 1458.02, 1350.31, 1296.82, 1248.84, 1107.23, 951.91, 846.73, 670.43, 568.11 cm^{-1}; ^{1}H NMR (400 MHz, $CDCl_3$, δ): 8.12-7.87 (m, 4H, H-1', H-2''' & H-6'''), 7.78 (d, *J* = 7.96 Hz, 3H, H-2'' & H-6''), 7.29 (d, *J* = 8.56 Hz, 3H, H-3''' & H-5'''), 7.10 (d, *J* = 8.52 Hz, 3H, H-3'' & H-5''), 5.28 (s, H-2'a), 5.15-5.12 (m, H-2a), 4.94-4.60 (m, 6H, H-1a & H-3a), 4.31-4.11 (m, 10H, H-α, H-α', H-1, H-3), 3.79-3.44 (m, 180H, -(OCH_2CH_2)$_{n\sim20}$), 2.68 (t, *J* = 7.96 Hz, 3H, H-1''''), 1.66 (q, *J* = 7.92 Hz, 3H, H-2''''), 1.40 (s, *J* = 7.32 Hz, 3H, H-3''''), 1.28 (t, *J* = 7.32 Hz, CH_3 of ethyl end group), 0.94 (t, J = 7.36 Hz, H-4''''); ^{13}C NMR (125.7 MHz, $CDCl_3$, δ): 170.2, 169.6, 169.4, 169.2, 169.2, 169.0 (-*C*OO-), 159.8, 159.6, 150.1, 145.1, 145.1, 131.4, 131.3, 128.3, 128.0, 127.8, 123.8, 121.8, 114.3, 70.1, 70.0, 69.7, 69.3, 68.1, 67.8, 67.7, 67.4, 67.0, 65.2, 64.3, 63.1, 62.9, 62.4, 61.8, 61.3, 60.7, 60.4, 60.2, 59.9, 57.8, 57.7, 50.9, 48.6, 34.7, 32.7, 31.1, 28.8, 28.5, 21.9, 21.5, 13.5, 13.2; $\overline{M}_n$ (NMR analysis) = 9404 g/mol; GPC (THF, 1 mL/min): $\overline{M}_w$ = 6510 g/mol, $\overline{M}_n$ = 4795 g/mol, PDI = 1.4.

Dendronized Polymer 4b (70 % Azobenzene and 30 % [G2.0] PG Dendron Functionalized). Compound **2** (0.31 mmol) (0.7 eq.) and compound **3** (0.15 mmol) (0.35 eq.) were used for synthesizing polymer **4b**, in a 1:1 mixture of dichloromethane and dimethylformamide, as a viscous oil in 85 % yield. IR (Neat): 3433.74, 2921.04, 2872.40, 1752.23, 1599.30, 1460.09, 1350.38, 1297.61, 1249.37, 1105.52, 951.52, 846.54, 719.79, 563.63 cm^{-1}; ^{1}H NMR (400 MHz, $CDCl_3$, δ): 8.04-7.88 (*m*, 4H, H-1', H-2''' & H-6''') 7.77 (d, *J* = 7.96 Hz, 3H, H-2'' & H-6''), 7.30 (d, *J* = 7.92 Hz, 3H, H-3''' & H-5'''), 7.10 (d, *J* = 8.56 Hz, 3H, H-3'' & H-5''), 5.28-5.13 (m, 4 H, H-2'a & H-2a), 4.94-4.59 (m, 8H, H-1a & H-3a), 4.21-4.11 (m, 9H, H-α, H-α' & H-2'b), 3.80-3.45 (m, 192H, -(OCH_2CH_2)$_{n\sim20}$), 2.69 (t, *J* = 7.92 Hz, 3H, H-1''''), 1.67 (q, *J* = 7.96 Hz, 3H, H-2''''), 1.42 (s, *J* = 7.32 Hz, 3H, H-3''''), 1.29 (t, *J* = 7.32 Hz, CH_3 of ethyl end group), 0.95 (t, *J* = 7.32 Hz, H-4''''); ^{13}C NMR (125.7 MHz, $CDCl_3$, δ): 169.8, 169.4, 169.1 (-*C*OO-), 159.8, 159.6, 150.2, 146.7, 146.6, 145.3, 145.3, 128.4, 123.9, 122.7, 121.9, 114.3, 70.3, 70.2, 69.8, 67.7, 67.7, 67.7, 62.7, 62.5, 61.9, 61.4, 60.8, 60.6, 57.8, 51.8, 51.1, 48.8, 34.9, 32.8, 31.2, 29.0, 28.7, 22.0, 21.6, 13.5, 13.3; $\overline{M}_n$ (NMR analysis) = 10612 g/mol; GPC (THF, 1 mL/min): $\overline{M}_w$ = 5960 g/mol, $\overline{M}_n$ = 4312 g/mol, PDI 1.4.

Results and discussion

The amphiphilic non-dendronized (**4a**) and dendronized (**4b**) polymers having equal proportions of azobenzene in the side chai

were synthesized by following the Novozym 435 catalyzed chemo-enzymatic approach followed by copper catalyzed "1,3-dipolar cycloaddition reaction". The synthesized polymers were fully characterized and explored for their encapsulation potential and release profile.

Synthesis and Characterization

The polymeric polyester structure was characterized completely by IR, ^{1}H, ^{13}C, ^{2}D HETCOR, and comparing the data with the already published results.[27] The degree of polymerization of the base co-polymer was calculated with ^{1}H NMR by end group analysis and compared with the GPC data. The $\overline{M}_n$ and $\overline{M}_w$ values of 10,583 and 13,579 g mol^{-1}, respectively, were obtained from GPC with polydispersity of 1.3 by using THF as a solvent and pullulan as standard (**Figure S9**). The degree of polymerization was found to be approximately 9 by both NMR and GPC results. The lower polydispersity (1.3 from GPC) of the co-polymer **1** compared to that given by Carother's equation' (PDI = 1.89) in the Novozym 435 catalyzed step-growth polymerization could be explained by the unique chain length or mass selectivity of the lipase.[27,45-48] The polymerization reaction carried out in bulk conditions also contribute to lower polydispersity as it increases in solvent-based polymerization reactions due to a greater rate of interchain transesterification reactions.[46] The constitution of 4'-butyl-4-propargyloxy(azobenzene) (**2**) was confirmed by both ^{1}H and ^{13}C NMR spectra (**Figure S13**). In ^{1}H NMR, the protons of the phenyl rings for *trans* and *cis* isomers of azobenzene appear separately with the protons of the *cis* isomer being slightly upfield compared to the protons of the former isomer (**Figures S13**). The integration of the peaks for the two isomers in ^{1}H NMR suggests the *trans*:*cis* ratio of 19:1 for 4'-butyl-4-propargyloxy(azobenzene) (**2**). The base polymer **1** was then functionalized with 4'-butyl-4-propargyloxy(azobenzene) (**2**) and propargylated [G2.0] PG dendron (**3**) to synthesize functionalized polymeric amphiphiles. The functionalization of the base co-polymer 'under Click regime' was monitored by the disappearance of azide peak at around 2109 cm^{-1} in the IR spectra and the product was confirmed by the observance of aromatic protons for the azobenzene and triazole moieties in the ^{1}H NMR spectrum (**Figures S14** and **S15**). The ^{13}C NMR spectrum also supported the formation of desired product by the observance of additional peaks in the aromatic region corresponding to 4'-butyl-4-propargyloxy(azobenzene) (**2**) and trizolyl carbons (**Figures S14** and **S15**). The triazole ring formation also resulted in the characteristic downfield shift for H-2 of glycerol from δ 3.89-3.98 ppm to δ 5.12-5.28 ppm and H-1 and H-3 of glycerol from δ 4.00-4.40 ppm to δ 4.59-4.94 ppm (**Figures S14** and **S15**). The ^{1}H, ^{13}C NMR spectra of 4'-butyl-4-propargyloxy(azobenzene) (**2**), both the polymeric amphiphiles (**4a** and **4b**) and ^{2}D HETCOR NMR spectra (**Figure S16**) of **4b** are given in SI.

Physico-chemical Characterization of Supramolecular Nano-structures

Both the dendronized (**4a**) and non-dendronized (**4b**) polymers having azobenzene in the side chain showed supramolecular aggregation behavior in the aqueous solution. The CAC of resulting nano-structures in aqueous solution was determined by fluorescence measurement using Nile red as a probe.[40] Dynamic light scattering measurements were used for determining t particle size.

Calculation of Critical Aggregation Concentration using Absorbance Measurement. The CAC of polymers was calculated by measuring the fluorescence intensity of encapsulated Nile red at different polymer concentrations. The fluorescence intensity of Nile red in blank solution (without polymeric amphiphile) was minimal at the studied dye concentration (4.7 x 10^{-6} M) and remained nearly constant below a specific concentration (CAC) of polymer and a substantial enhancement in intensity was observed above it reflecting the dye encapsulation within the micellar nano-structures. CAC is thus calculated by plotting the fluorescence intensity of Nile red at 636 nm against log [polymer concentration] (**Figure 1**).

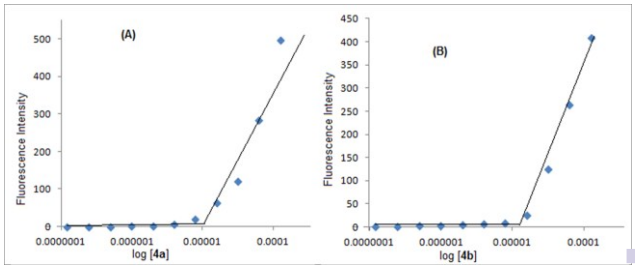

Figure 1. (A) Plot of fluorescence intensity vs log [**4a**]; (B) plot of fluorescence intensity vs log [**4b**] for calculating the critical aggregation concentration.

The CAC of non-dendronized polymer **4a**, was found to be 1.07 x 10^{-5} M while that of its dendronized analog **4b** increases to 1.66 x 10^{-5} M. A similar behavior was also observed in our earlier report [a

polymeric systems having hydrophobic alkyl chain and polyglycerol based dendrons.[26]

Dynamic Light Scattering and Cryo-TEM Measurements. The supramolecular aggregation tendency of the polymers was explored in aqueous solution at the concentration of 10 mg/mL. The size of the most prominent nano-particles in the aqueous solution of polymer **4a** and **4b** was 9.3 and 9.7 nm in volume with polydispersity values of 0.473 and 0.416, respectively above their CAC (**Figure S11**). A trimodal distribution in intensity was observed, however, it was monomodal only, in terms of volume and number indicating that the smallest size particles in intensity are the most prominent species in their aqueous solution and hence are the only peaks in volume and number. Below the CAC, the peak distribution was monomodal in all the three modes i.e. intensity, volume and number indicating only one kind of species in the aqueous solution. The effect of *trans-cis* isomerization on particle size was also studied for polymer **4a** below CAC, with a size of 384 and 280 nm with polydispersities of 0.219 and 0.201 for *trans* and *cis* forms respectively (**Figure S12**). The cryo-TEM of polymer **4a** at the concentration of 10 mg/ml also indicated the uniform distribution of spherical nano-particles in the range of 7-15 nm (**Figure 2**).

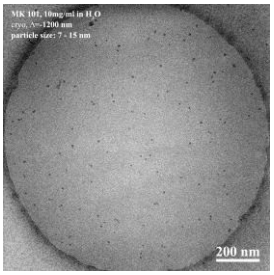

Figure 2. Cryo-TEM image of polymer **4a**, representing the spherical nanoparticles in the range of 7-15 nm.

Photo-isomerization Behavior

The UV-visible absorption spectra of the polymeric systems, in the *trans* isomer exhibit bands at 242, 351 and 440 nm for π-π* transitions localized on phenyl ring, symmetry allowed π-π* transitions delocalized throughout the molecule, including the two nitrogen atoms, and symmetry-forbidden n-π* transitions occurring at the central nitrogen atoms, respectively (**Figures 3, 4, S1** and **S2**).[9,39] On the other hand, in *cis* form π-π* transitions involving the two nitrogen atoms exhibit a blue shift to 263 nm, however the prominent n-π* transitions at central nitrogen atoms remain localized at 440 nm (**Figures 3, 4, S1** and **S2**).

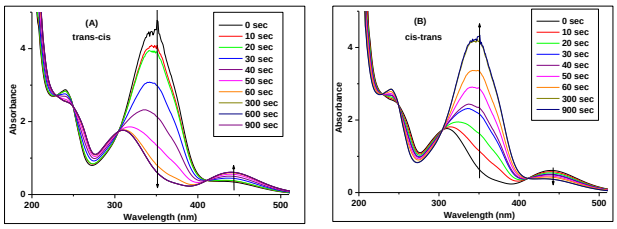

Figure 3. Photoisomerization of polymer **4a** in aqueous solution above critical aggregation concentration, **(A)** Irradiation at 365 nm (*trans-cis*); **(B)** Irradiation at 254 nm (*cis-trans*).

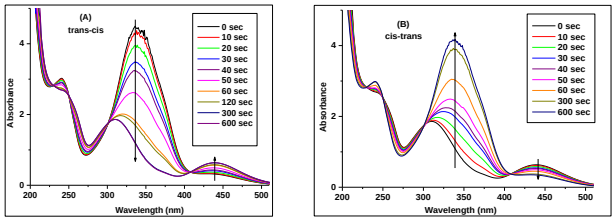

Figure 4. Photoisomerization of polymer **4b** in aqueous solution above critical aggregation concentration, **(A)** Irradiation at 365 nm (*trans-cis*); **(B)** Irradiation at 254 nm (*cis-trans*).

In the UV absorption spectrum of polymer **4b** above its CAC, the delocalized π-π* transitions in *trans* form get slightly blue-shifted to 337 nm (**Figure 4**). This blue-shift could be explained owing to the more non-polar environment when inserted in the hydrophobic core,[5,31,49] of the resulting micellar aggregates because of [G2.0] PG dendrons on the outer surface which acts as a shield to the azobenzene moieties in the core from the aqueous environment. Photoisomerization of an aqueous solution of azobenzene functionalized polymers **4a** and **4b** was carried both above and below their CAC to study the effect of *trans-cis* isomerization on the micellar aggregates, using a 6 W mercury lamp. The *trans* isomers could be isomerized to *cis* form on irradiating π-π* transitions with 365 nm light while the reverse *cis-trans* isomerization could be acheived either by allowing the *cis* isomer dominated samples to stay in darkness (thermal isomerization),[7] owing to higher stability of trans isomers over *cis* or irradiating the n-π* transitions with visible light (400-500 nm),[5] or π-π* transitions with UV light (250-270 nm),[9] of the *cis* azobenzene. The *trans-cis* isomerization was studied by irradiating with the light of 365 nm as the molar absorptivity of the *trans* isomer is much higher than the later one[5] at this wavelength. *Trans* to *cis* isomerization led to a decrease in the intensity of the absorbance band at 351 and 337 nm for polymers **4a** and **4b** respectively, and an increase in the intensity of absorbance bands at 263 and 440 nm untill a photostationary state

is reached. The *trans-cis* photoisomerization above CAC occurs at a faster rate in polymer **4a** (**Figure 3A**) as its photostationary state is reached in approximately 60 seconds, while it takes 300 seconds for polymer **4b** (**Figure 4A**). The rapid of *trans-cis* photoisomerization of polymer **4a** as compared to **4b** may be due to more steric hindrance and embedding of azobenzene moieties,[5] within the core of micelles in **4b**, which is also supported by the observance of blue shift of 14 nm for its π-π* absorption maxima as compared to **4a**. A reverse isomerization i. e., *cis-trans* was observed on irradiating the polymer solutions at 254 nm,[9] this is accompanied by the enhancement in intensity of the absorbance band at 351 and 337 nm for polymer **4a** and **4b** respectively and decrease in the intensity of absorbance bands at 263 and 440 nm. After irradiation of the *cis* isomer at 254 nm above the CAC, approximately 95 % of initial absorbance for π-π* transitions of azobenzene in *trans* form was recovered, indicated the efficient reversible isomerization in 300 and 600 seconds for polymers **4a** and **4b** respectively (**Figures 3B** and **4B**). A thermal isomerization of the *cis* isomer was also observed on keeping in darkness for 24 h or more. The rate of *cis-trans* isomerization was found to be comparable for both polymers. The photoisomerization rates were also compared in terms of their rate constants (SI).[31,32] The rate of photoisomerization increases significantly below CAC (SI). This can be explained by the fact that the azobenzene moieties get embedded in the interior core of the micellar structure above their CAC which limits their mobility and also lowers the free volume availability, both of these factors are reported to be crucial for efficient isomerization.[5,50] A similar observation has been made by Lo *et al.*,[32] while studying the azobenzene moiety based micelles in organic solvent.

Encapsulation Potential

The encapsulation potential of polymeric systems was explored using the Nile red and curcumin as model guest molecules. The encapsulation of curcumin was done qualitatively only since the absorbance spectrum of curcumin was overlapping with that of the polymer.

Nile red Encapsulation. Nile red is a hydrophobic and a solvatochromic fluorescent dye which is very commonly used for evaluating the transport potential of nanocarriers. Furthermore, the selection of Nile red as a model dye for encapsulation facilitates the measurement of contribution of additional π-π interactions by comparing the encapsulation potential of these polymers with the non aromatic polymeric systems synthesized earlier by our group.[26]

The polymeric systems reported previously from our group were also based on identical base co-polymer (**1**), however, it was functionalized further with varied length alkyl chains (C_{12}/C_{14}) as hydrophobic component in spite of azobenzene moieties in the side chain. The ratio of the hydrophobic alkyl group and hydrophilic PG dendron used herein has been kept identical to the previous study for better comparison. The encapsulation was studied at a dye concentration of 0.4 mM in 1 mg per ml of polymer solution by following the protocol published earlier from our group (**Figure 5**).[26]

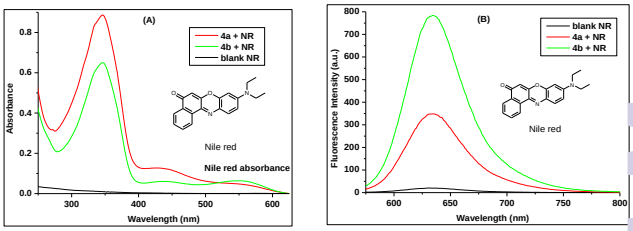

Figure 5. **(A)** UV absorbance spectra of Nile red encapsulated samples in methanol; **(B)** Fluorescence spectra of Nile red encapsulated samples in methanol.

The dendronized polymer **4b** exhibits better transport potential as compared to the non-dendronized analog (**4a**) with encapsulation efficiency of 1.87 and 1.45 %, respectively. The transport efficiency of dendronized polymer **4b** was found to be 7 and 3 times to the transport efficiency of corresponding dendronized polymers having C_{12} and C_{14} alkyl chain and [G2.0] PG dendron respectively.[26] The higher encapsulation potential of azobenzene functionalized dendronized polymers compared to alkyl chain (C_{12}/C_{14}) funtionalized polymers could be explained due to additional π-π interactions between the azobenzene moieties in the core of micellar aggregates and the guest molecule (Nile red).

Curcumin Encapsulation. Curcumin possesses a number of therapeutic properties such as anticancer,[51] antimicrobial,[52] antioxidant,[53] anti-inflammatory,[54] and various others, but its low aqueous solubility and high chemical and photochemical instability leads to poor bioavailability.[55] A number of attempts have been made to increase the bioavailability of curcumin by encapsulating it in liposomes,[56] polymeric,[57] or surfactant micelles,[58] cyclodextrin,[59] hydrogels,[60] and other nanocarriers, but these systems were found to have their own limitations. We attempted to encapsulate curcumin using our polymeric systems. Both the polymers **4a** and **4b** were able to encapsulate curcumin as shown by the high fluorescence intensity of curcumin after encapsulation as compared

to that in the blank aqueous solution (**Figure S10**). The polymer **4b** was observed to exhibit improved encapsulation potential in comparison to **4a**.

Photoinduced Release Profile of Nile red

Since the polymeric systems having the azobenzene moieties in the side chain exhibit the rapid geometrical isomerization on UV irradiation in their aqueous solution, herein we explored the effect of such reversible isomerization on release potential of encapsulated guest (Nile red). The amphiphilic polymers organize themselves into micellar structures in the aqueous solution with the azobenzene moieties directed in the interior core and hydrophilic PEG facing aqueous layer in the case of polymer **4a** and [G2.0] polyglycerol dendrons forming a corona on the outer surface in case of polymer **4b**. On isomerization of the *trans* azo moiety into *cis* by irradiation at 365 nm, the size of the internal cavity of the micellar structure changes along with the increase in dipole moment, which in turn lowers the encapsulation of hydrophobic moieties in the core, thus affecting the encapsulation capacity of the polymers. We have studied the effect of this geometrical isomerization on the polymeric aqueous solutions with the encapsulated Nile red in their micellar core by using fluorescence spectroscopy as per literature reports.[33-38] Nile red is a photochromic and hydrophobic moiety and its fluorescence intensity is known to increase in the hydrophobic environment.[29,30] Due to higher thermodynamic stability of *trans* isomer, the azobenzene moiety exists predominantly in the *trans* form in the polymer. On irradiating the Nile red encapsulated sample of the polymers at 365 nm and subsequently recording the fluorescence intensity at regular intervals, it was observed that the dye intensity keeps on decreasing with the gradual conversion of *trans* azobenzene moieties into *cis* and becomes nearly static after 60 seconds (**Figures 6A** and **7A**).

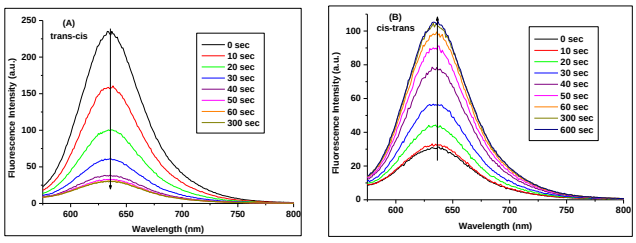

Figure 6. Photo-induced release of Nile red from polymer **4a** as is shown by a net decrease in fluorescence intensity, **(A)** Irradiation at 365 nm causes *trans-cis* isomerization with a decrease in fluorescence intensity of Nile red; **(B)** Irradiation at 254 nm causes *cis-trans* isomerization with an increase in fluorescence intensity of Nile red leading to partial regain.

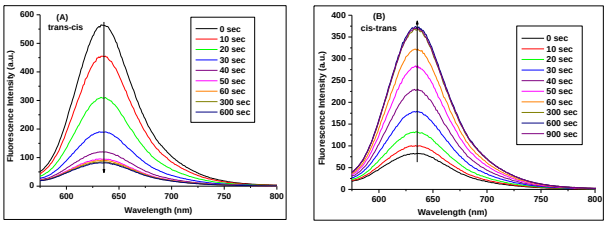

Figure 7. Photo-induced release of Nile red from polymer **4b** as is shown by a net decrease in fluorescence intensity, **(A)** Irradiation at 365 nm causes *trans-cis* isomerization with a decrease in fluorescence intensity of Nile red; **(B)** Irradiation at 254 nm causes *cis-trans* isomerization with an increase in fluorescence intensity of Nile red leading to partial regain.

This decrease in the fluorescence intensity could be explained partially by the release of dye from the core of micellar structures into the aqueous solution due to changes in the size and shape of internal core and partially by the increase in the polarity of the core resulting from the conversion of *trans* isomer into *cis*.[33,34] However, on irradiating the polymer, predominant with the *cis* form, with 254 nm light, the fluorescence intensity of Nile red was observed to increase partially suggesting that dye is now available in the more hydrophobic microenvironment because of a decrease in the dipole moment of internal core as a result of reconversion of *cis* isomers into *trans* (**Figures 6B** and **7B**).[33,34,36] However, a complete regain of the fluorescence intensity of Nile red could not be observed and this may be because some of dye molecules might have been released from the internal cavity due to change in its size and shape into the aqueous medium and thus could not be pushed back completely into the hydrophobic core. The rate of re-encapsulation of released Nile red from the aqueous solution into the micellar core is slow as compared to the rate of *cis-trans* isomerization process.[37] Thus, this reduced fluorescence intensity on *trans-cis-trans* reverse isomerization marks the net release of Nile red molecules form micellar structures. The % release of Nile red was calculated by measuring the fluorescence intensity before and after *trans-cis-trans* reverse isomerization, and found to be approximately 50 ± 5 and 29 ± 5 % for polymers **4a** and **4b** respectively on completion of 1st photocycle. The relatively higher release of dye by polymer **4a** as compared to **4b** could be explained due to more rapid and efficient *trans-cis* isomerization in case of polymer **4a** above the CAC compared to **4b** due to the absence of bulkier [G2.0] PG dendrons corona on the outer surface of micellar

structures in the case of polymer **4a**. The method and data used for the calculation of % release using fluorescence measurements is given in SI. The effect of the geometrical isomerization of azomoiety incorporated in the polymeric system was also studied by applying the photo-cycling process for non-dendronized polymer **4a**. The isomerization of *trans* isomers into *cis* and then its re-conversion back to *trans*, thus constitute one photo-cycle. The further repetition of photocycles without allowing any thermal restoration does not lead to any further release of Nile red (**Figures 8, S4 and S6**). However, on keeping the Nile red encapsulated samples for thermal restoration in dark after performing one or more photocycles, led to a net increase in the intensity of Nile red (**Figures 8, 5A and 7A**), this could be attributed to the partial re-encapsulation of dye from the aqueous environment into the miceller core. Thus, performing the photocycles by allowing a thermal restoration in dark for more than 2 h, (**Figures 8, S5 and S7**) led to a net release of Nile red, of the same magnitude (40-50%) as observed in 1st photo-cycle (**Figure S3**). The % cumulative release of Nile red as a function of photoisomerization cycles with different thermal restoration time intervals is given in **Figure 8**, which is calculated from the fluorescence intensity of Nile red as in **Figures S3-S7**, for polymer **4a**.

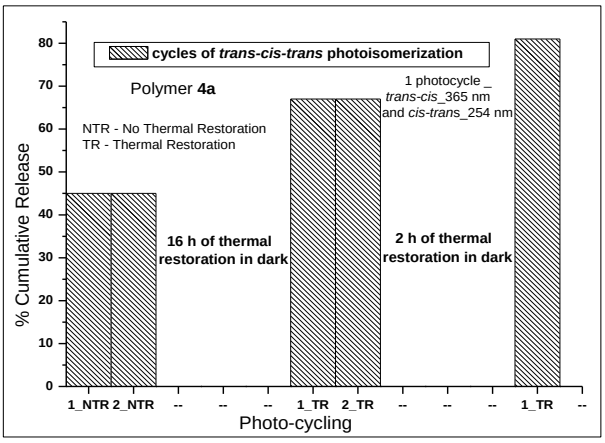

Figure 8. % Cumulative release of Nile red for polymer **4a** as a function of different photocycles with/without variable thermal restoration time intervals (2/16 h).

Conclusions

We have synthesized polyester based linear polymers using PEG diester and azido glycerol by following a 'Bio-catalytic' approach. The post-functionalization of these linear co-polymers with azobenzene only or azobenzene and polyglycerol dendrons via 'Click approach' resulted in non-dendronized and dendronized "Photoresponsive Polymeric Amphiphiles" respectively. Both, the dendronized and non-dendronized polymers were completely characterized by IR, GPC, DLS, ^{1}H & ^{13}C NMR and UV spectroscopy. The polymeric amphiphiles have shown a good encapsulation tendency for model hydrophobic guest candidates (curcumin and Nile red). The photoisomerization behavior was studied for the aqueous solution of the polymers, both above and below CAC. The rate of *trans-cis* isomerization below CAC was found to be approximately 4 times higher for polymer **4a** while it is 7 times higher for **4b** as compared to above CAC values while the rate of *cis-trans* isomerization below CAC was found to be approximately 11 times higher for polymer **4a** while it is 14 times higher for **4b** as compared to above the CAC value. The effect of photoisomerizati was also studied for Nile red encapsulated samples above CAC by using fluorescence spectroscopy and the photoresponsive release of Nile red was observed from the micellar aggregates. A dependence of Nile red release on the thermal restoration of *cis-trans* isomerization has also been observed. The dendronized polymer **4b** has shown higher encapsulation efficiency for Nile red while the photoresponsive release of Nile red was higher in polymer **4a**. These results suggest that the azobenzene moieties are responsible for the photoresponsive release and [G2.0] PG dendrons increase the stability of micellar aggregates and enhance their encapsulation potential.

Acknowledgements

We would like to acknowledge IGSTC (Indo-German Science and Technology Center) and DST (Department of Science and Technology)-Purse Grant Phase-II for providing the funds for carrying out the research work. We also would like to thank CSIR, India (Council of Scientific and Industrial Research) for providing junior and senior research fellowships to Ms. Meena Kumari.

Notes and references

1. Q. Yan, J. Y. Yuan, Y. Kang, Z. N. Cai, L. L. Zhou and Y. W. Yin, *Chem. Commun.*, 2010, 46, 2781-2783.
2. A. Kikuchi and T. Okano, *Prog. Polym. Sci.*, 2002, **27**, 1165-1193.

3. L. Peng, M. You, C. Wu, D. Han, I. €Oc-soy, T. Chen, Z. Chen and W. Tan, *ACS NANO*, 2014, **8**, 2555-2561.
4. W. Yuan, J. Shen and W. Guo, *Mater. Lett.*, 2014, **134**, 259-262.
5. Z. Cui, T. Phoeung, P. Rousseau, G. Rydzek, Q. Zhang, C. G. Bazuin and M. Lafleur, *Langmuir*, 2014, **30**, 10818-10825.
6. A. Diguet, M. Yanagisawa, Y. J. Liu, E. Brun, S. Abadie, S. Rudiuk and D. Baigl, *J. Am. Chem. Soc.*, 2012, **134**, 4898-4904.
7. E. Blasco, J. L. Serrano, M. Piñol and L. Oriol, *Macromolecules*, 2013, **46**, 5951-5960.
8. M. Shimomura and T. Kunitake, *J. Am. Chem. Soc.*, 1987, **109**, 5175-5183.
9. N. Drillaud, E. Banaszak-Léonard, I. Pezron and C. Len, *J. Org. Chem.*, 2012, **77**, 9553-9561.
10. C. Kordel, S. Popeney and R. Haag, *Chem. Commun.*, 2011, **47**, 6584-6586.
11. R. H. El-Halabieh, O. Mermut and C. J. Barrett, *Pure Appl.Chem.*, 2004, **76**, 1445-1465.
12. K. Yamaguchi, S. Kume, K. Namiki, M. Murata, N. Tamai and H. Nishihara, *Inorg. Chem.*, 2005, **44**, 9056-9067.
13. M. Quick, A. L. Dobryakov, M. Gerecke, C. Richter, F. Berndt, I. N. Ioffe, A. A. Granovsky, R. Mahrwald, N. P. Ernsting and S. A. Kovalenko, *J. Phys. Chem. B*, 2014, **118**, 8756-8771.
14. E. Blasco, J. Barrio, M. Piñol, L. Oriol, C. Berges, C. Sánchez and R. Alcalá, *Polymer*, 2012, **53**, 4604-4613.
15. D. Bleger, T. Liebig, R. Thiermann, M. Maskos, J. P. Rabe and S. Hecht, *Angew. Chem., Int. Ed.*, 2011, **50**, 12559-12563.
16. S. Lin, Y. Wang, C. Cai, Y. Xing, J. Lin, T. Chen and X. He, *Nanotechnology*, 2013, **24**, 085602/1-085602/10.
17. X. Xue, J. Zhu, Z. Zhang, N. Zhou, Y. Tu and X. Zhu. *Macromolecules*, 2010, **43**, 2704-2712.
18. X. Kang, J. Zhao, H. Li and S. He, *Colloid Polym. Sci.*, 2013, **291**, 2245-2251.
19. Z. Li, Y. Zhang, L. Zhu, T. Shen and H. Zhang, *Polym. Chem.*, 2010, **1**, 1501-1511.
20. K. Watari and H. Kouzai, *Polym. J.*, 2006, **38**, 298-301.
21. P. Forcén. L. Oriol, C. Sánchez, F. J. Rodríguez, R. Alcalá, S. Hvilsted and K. Jankova, *Eur. Polym. J.*, 2007, **43**, 3292-3300.
22. S. K. Sharma, M. Husain, R. Kumar, L. A. Samuelson, J. Kumar, A. C. Watterson and V. S. Parmar, *Pure Appl. Chem.*, 2005, **77**, 209-226.
23. S. K. Sharma, R. Kumar, S. Kumar, R. Mosurkal, V. S. Parmar, L. A. Samuelson, A. C. Watterson and J. Kumar, *Chem. Commun.*, 2004, 2689-2691.
24. S. Gupta, M. K. Pandey, K. Levon, R. Haag, A. C. Watterson, V. S. Parmar and S. K. Sharma, *Macromol. Chem. Phys.*, 2010, **211**, 239-244.
25. S. Gupta, B. Schade, S. Kumar, C. Böttcher, S. K. Sharma and R. Haag, *Small*, 2013, **9**, 894-904.
26. M. Kumari, A. K. Singh, S. Kumar, K. Achazi, S. Gupta, R. Haag and S. K. Sharma, *Polym. Adv. Technol.*, 2014, **25**, 1208-1215.
27. M. Kumari, S. Gupta, K. Achazi, S. Stefani, C. Böttcher, J. Khandare, S. K. Sharma, R. Haag, *Macromol. Rapid Commun.* 2015, **36**, 254-261.
28. R. Huisgen, *Angew. Chem., Int. Ed*., 1963, **2**, 565-598.
29. A. Y. Jee, S. Park, H. Kwon and M. Lee, *Chem. Phys. Lett.*, 2008, **477**, 112-115.
30. I. N. Kurniasih, H. Liang, S. Kumar, A. Mohr, S. K. Sharma, J. P. Rabe and R. Haag, *J. Mater. Chem. B*, 2013, **1**, 3569-3577.
31. X. Xue, J. Zhu, W. Zhang, Z. Zhang, X. Zhu, *Polymer*, 2009, **50**, 4512-4519.
32. S. Tsao, C. Lo, *RSC Adv.*, 2014, **4**, 23585-23594.
33. E. Blasco, J. L. Serrano, M. Piñol and L. Oriol, *Macromolecules*, 2013, **46**, 5951-5960.
34. E. Blasco, B. V. K. J. Schmidt, C. Barner-Kowollik, M. Piñol and L. Oriol, *Macromolecules*, 2014, **47**, 3693-3700.
35. C. Park, J. Lim, M. Yun and C. Kim, *Angew. Chem., Int. Ed.*, 2008, **47**, 2959-2963.
36. Z. Feng, L. Lin, Z. Yan and Y. Yu, *Macromol. Rapid Commun.*, 2010, **31**, 640-644.
37. S. Menon, R. M. Ongungal and S. Das, *Macromol. Chem. Phys.*, 2014, **215**, 2365-2373.
38. D. Hu, Y. Li, Y. Niu, L. Li, J. He, X. Liu, X. Xia, Y. Lu, Y. Xiong and W. Xu, *RSC Adv.*, 2014, **4**, 47929-47936.
39. F. Hamon, F. Djedaini-Pilard, F. Barbot, C. Len, C. *Tetrahedron*, 2009, **65**, 10105-10123.
40. A. C. Rodrigo, A. Barnard, J. Cooper, D. K. Smith, *Angew. Chem., Int. Ed.*, 2011, **50**, 4675-4679.
41. V. Kumar, B. Gupta, G. Kumar, M. K. Pandey, E. Aiazian, V. S. Parmar, J. Kumar, A. C. Watterson, *J. Macromol. Sci., Pure Appl. Chem.*, 2010, **47**, 1154-1160.
42. E. Fleige, B. Ziem, M. Grabolle, R. Haag, U. Resch-Genger, *Macromolecules*, 2012, **45**, 9452-9459.

43. T. G. Barclay, K. Constantopoulos, W. Zhang, M. Fujiki, J. G. Matisons, *Langmuir*, 2012, **28**, 14172-14179.
44. M. Wyszogrodzka, R. Haag, *Chem. Eur. J.*, 2008, **14**, 9202-9214.
45. F. Binns, P. Harffey, S. M. Roberts, A. Taylor, *J. Polym. Sci., Part A: Polym. Chem.*, 1998, **36**, 2069-2080.
46. A. Mahapatro, B. Kalra, A. Kumar, R. A. Gross, *Biomacromolecules*, 2003, **4**, 544-551.
47. S. S. Müller, H. Frey, *Macromol. Chem. Phys.*, 2012, **213**, 1783-1790.
48. H. Uyama, K. Inada, S. Kobayashi, *Polym. J.*, 2000, **32**, 440-443.
49. X. Song, J. Perlstein, D. G. Whitten, *J. Am. Chem. Soc.*, 1997, **119**, 9144-9159.
50. M. Shimomura, T. Kunitake, *J. Am. Chem. Soc.*, 1987, **109**, 5175-5183.
51. A. Duvoix, R. Blasius, S. Delhalle, M. Schnekenburger, F. Morceau, E. Henry, M. Dicato, M. Diederich, *Cancer Lett.*, 2005, **223**, 181-190.
52. H. H. Tønnesen, H. de Vries, J. Karlsen, G. Beijersbergen van Henegouwen, *J. Pharm. Sci.*, 1987, **76**, 371-373.
53. R. M. N. Sreejayan, *J. Pharm. Pharmacol.*, 1997, **49**, 105-107.
54. I. Brouet, H. Ohshima, *Biochem. Biophys. Res. Commun.*, 1995, **206**, 533-540.
55. P. Anand, A. B. Kunnumakkara, R. A. Newman and B. B. Aggarwal, *Mol. Pharm.*, 2007, **4**, 807-818.
56. A. Kunwar, A. Barik, R. Pandey and K. I. Priyadarsini, *Biochim. Biophys. Acta*, 2006, **1760**, 1513-1520.
57. L. Liu, L. Sun, Q. Wu, W. Guo, L. Li, Y. Chen, Y. Li, C. Gong, Z. Qian and Y. Wei, *Int. J. Pharm.*, 2013, **443**, 175-182.
58. H. H. Tønnesen, *Pharmazie*, 2002, **57**, 820-824.
59. K. N. Baglole, P. G. Boland and B. D. Wagner, *J. Photochem. Photobiol., A*, 2005, **173**, 230-237.
60. W. Wu, J. Shen, P. Banerjee and S. Zhou, *Biomaterials*, 2011, **32**, 598-609.